Functional analysis of DCAF7 and ERCC1-XPF interaction identified by affinity-purification and mass spectrometry

doi: https://doi.org/10.1016/j.bbrc.2019.08.147

Chapter 1 Identification of interacting factors with ERCC1-XPF

1-1. Introduction

DNA damage response

Our genomic DNA is constantly exposed to various kinds of DNA damaging factors, which can be exogenous and endogenous, such as ultraviolet (UV) light, ionizing radiation, reactive oxygen species, and replication stresses (Friedberg et al., 2006). If such DNA damage are not properly processed, they will cause mutations, cellular senescence, death, and oncogenesis. To prevent from developing those harmful consequences and maintain DNA sequence integrity, our cells have multiple DNA damage response pathways; mismatch repair (MMR), nucleotide excision repair (NER), base excision repair (BER), interstrand crosslink repair (ICL), homologous recombination (HR), non-homologous end-joining (NHEJ) and so on (Bouwman et al., 2012). Analysis of the detailed mechanisms of DNA damage response would provide us with promising ways for prevention and treatment of many diseases, including cancer.

UV-induced photolesions and nucleotide excision repair

Nucleotide excision repair (NER) is a major mechanism for repairing dimeric pyrimidine photolesions by ultraviolet light or bulky chemical base adducts. The major UV photoproducts are the cyclobutane pyrimidine dimers (CPD) and (6-4) photoproducts (6-4PP) (Friedberg et al., 2006; Schärer, 2013). The biochemical mechanism of NER has been well characterized, which includes damage recognition, dual incisions, release of excised oligonucleotides, repair synthesis to fill the gap and ligation (Hu et al., 2017; Adebali et al., 2017a; Adebali et al., 2017b; Li et al., 2018) (Fig. 2).

Deficiency in the NER is related to a rare hereditary disease, xeroderma pigmentosum (XP), which is classified into seven XP complementation groups, A (XP-A) through G (XP-G) (Friedberg et al., 2006; Cleaver et al., 2009). All seven responsible genes were already identified and are known to code proteins essential or sub-essential for NER reaction. XP patients are characterized by photosensitivity, pigment changes and a predisposition to skin cancer on areas exposed to sun light, which are potentially caused by their inability to repair UV-induced DNA lesions.

ERCC1-XPF heterodimer essential for NER

ERCC1-XPF is one of the indispensable NER factors, which is involved in not only NER, but also other DNA repair systems, including ICL repair (De Silva et al., 2000; Kuraoka et al., 2000; De Silva et al, 2002; Niedernhofer et al., 2004; Fisher et al., 2008; Klein et al., 2014), HR (Sargent et al., 1997; Adair et al., 2000; Ahmad et al., 2008; Al-Minawi et al., 2008; Bennardo et al., 2008). The ERCC1-XPF complex is a structure specific endonuclease, which makes a nick at the junction of double-stranded to single-stranded DNA transition with a polarity of 5' to 3' direction (Matsunaga et al., 1996; Sijbers et al., 1996; de Laat et al., 1998a). As a result, DNA substrates for this endonuclease contain a special structure such as a splayed arm, stem loop, bubble, or 3' flap (Fig. 2B). ERCC1 and XPF interact with each other via their C-terminal helix-hairpin-helix (HhH) regions (de Laat et al., 1998b) (Fig. 2A). XPF protein contains a catalytic domain, although the structural support of ERCC1 is required for its endonuclease activity (Fig. 1A and B) (Enzlin and Scharer 2002; Tripsianes et al., 2005).

Pathology associated with ERCC1-XPF malfunction

In humans, germline mutations in both alleles of *XPF/ERCC4* gene causes not only

XP complementation group F (shortly XP-F), but also other severer genetic disorders, XFE progeroid syndrome, Fanconi anemia (FA), Cockayne syndrome (CS) and a combined form of XP/CS (Gregg et al., 2011; Manandhar et al., 2015). In contrast, no *ERCC1* mutations have been identified in XP patients so far. It was recently reported that one of the patients suffered from cerebro-oculo-facio-skeletal (COFS) syndrome harbors mutations in *ERCC1* gene (Kashiyama et al., 2013). This patient manifested severe developmental failure, microcephaly and skeletal abnormalities. In mouse models, two *ERCC1* knockout strains were independently generated by two groups (McWhir et al., 1993; Weeda et al., 1997), and showed severe growth failure and nuclear abnormality and died at approximately 3 weeks before weaning. The mice lacking ERCC1 also developed various symptoms including progressive neurodegeneration, rapid turnover of hematopoietic cells, musculo-skeletal and nervous system defects, and impaired liver function (Núñez et al., 2000; Niedernhofer et al., 2006). Taken together, it is clear that the normal function of ERCC1-XPF is important for not only cancer prevention but also normal development as well as the suppression of neurodegeneration.

Cellular levels of ERCC1-XPF

The heterodimer formation of ERCC1 and XPF is also known to be also necessary for their stability (Biggerstaff et al., 1993; Reardon et al., 1993; van Vuuren et al., 1993). XP-F patients carry a missense mutation in at least one allele of *XPF/ERCC4* genes (Gregg et al., 2011; Manandhar et al., 2015) and show only marginal or undetectable level of XPF protein, whereas ERCC1 protein level is also markedly reduced in various XP-F cell strains (Yagi et al., 1997). Similarly, *ERCC1*-mutated cells showed low XPF level (Jaspers et al., 2007) and ERCC1 knockdown caused the significant reduction of XPF protein level without affecting mRNA level (Arora et al., 2010). It has been also shown that ERCC1 can fold only in the presence of XPF *in vitro,* suggesting that XPF acts as a scaffold for the proper folding of ERCC1 (Tripsianes et al., 2005; Choi et al., 2005). In addition, the cellular level of ERCC1-XPF is well known to influence the efficacy of platinum-based cancer chemotherapy. However, the detailed mechanism of how the cellular levels of ERCC1 and XPF is regulated still remains elusive.

Objective of this study

In this study, I set a goal to identify novel interacting factors with ERCC1-XPF and uncover their functions to obtain the information regarding regulatory mechanisms of ERCC1-XPF. At Chapter 1, I have tried to identify novel interacting factors with ERCC1-XPF using Flp-In T-REx 293 cells conditionally expressing FLAG- and 6xHis-tagged ERCC1 or XPF and tandem purification followed by mass spectrometry. I obtained 699 candidates from the fractions and found 14 kinds of E3 ligases and 5 kinds of deubiquitinases included. After immunoprecipitation experiments and subsequent siRNA-mediated knockdown experiments, I found that DCAF7 and USP11 are novel interacting proteins with ERCC1-XPF and their knockdown affects cellular protein levels of ERCC1-XPF. At Chapter 2, I have focused on the functional analysis of DCAF7 and ERCC1-XPF interaction and found that DCAF7 is a novel regulator for maintaining the cellular level of ERCC1-XPF and NER activity.

1-2. Results

Overexpression of double-tagged ERCC1 or XPF and their tandem affinity purification.

To explore a novel interacting protein(s) of ERCC1-XPF, I employed affinity purification and mass spectrometry using Flp-In T-REx 293 cells conditionally expressing FLAG- and 6xHis-tagged ERCC1 or XPF upon the treatment of tetracycline or its derivatives. The cell lines were established by Dr. Joyce T. Reardon, and were kindly provided by Dr. Aziz Sancar, University of North Carolina at Chapel Hill, USA. The two cell lines and their parental cells (negative control) were treated with tetracycline for 48 h and each proteins were visualized by immunoblotting (Fig. 3A). I could detect overexpressed double-tagged ERCC1 or XPF, which are much higher levels compared to the endogenous ERCC1 or XPF. Furthermore, the endogenous ERCC1 was downregulated and almost depleted due to the overexpression of FLAG-ERCC1-6xHis. Next, I optimized tandem purification of those bait proteins by first Ni-NTA agarose and subsequent anti-FLAG antibody resin, and found the condition under which FLAG-ERCC1-6xHis can be efficiently isolated (Fig. 3B). I validated the interaction between overexpressed FLAG-ERCC1-6xHis and endogenous XPF or ectopic FLAG-XPF-6xHis and endogenous ERCC1 using co-immunoprecipitation experiments (Fig. 3C). Finally,

I visualized all proteins in each sample by silver staining to check how abundant non-specific proteins are included (Fig. 3D). After the first Ni-NTA purification, there are still many bands detected in the sample from parental cells, indicating that the fractions contains non-specific proteins (Lane 2). After the subsequent anti-FLAG antibody resin purification, however, most of non-specific bands were eliminated and only a few bands were visible (Lane 3). Additionally, a strong signal was observed at the estimated molecular size 103 kDa in FLAG-ERCC1-6xHis fraction (Lane 7) or at the estimated band size 36 kDa in FLAG-XPF-6xHis fraction, suggesting the detection of endogenous XPF or ERCC1 co-purified, respectively. More importantly, in both tandem-purified fractions, there were many other bands which were not seen in the fraction of parental cells (Lane 3 vs 7). I concluded that the fractions after the tandem purification would be applicable to mass spectrometry analysis.

List of ERCC1- or XPF-interacting factors identified by mass spectrometry analysis

I submitted the purified fractions to the UNC Michael Hooker Proteomics Center, University of North Carolina at Chapel Hill (USA) for mass spectrometry. In total, polypeptides from 699 proteins were detected, which include several

proteins previously reported to interact with ERCC1-XPF, XPA, MSH2 and SLX4 (Park and Sancar, 1994; Lan et al., 2004; Muñoz et al., 2009), indicating that the purification and mass spectrometry were properly conducted for our purposes. On the other hand, RPA (a known XPF interactor) and USP45 (a known ERCC1 interactor) (de Laat et al., 1998; Perez-Oliva et al., 2015) were not detected. The lists include many proteins related to the ubiquitination/deubiquitination system, DNA replication, molecular chaperons, heat shock proteins, ribosomal proteins and so on (data not shown). In particular, I was interested in the proteins related to the ubiquitination/deubiquitination system, since they are possibly implicated in the regulation of ERCC1-XPF stability. In this category, 14 kinds of E3 ubiquitin ligases and 5 kinds of deubiquitinases were included (Table 1).

Validation of each interaction by transient co-expression and co-immunoprecipitation.

Mass spectrometry is very powerful and sensitive, but often includes false-positive proteins. I next carried out co-immunoprecipitation experiments by overexpressing epitope-tagged candidate interactors along with tagged or non-tagged ERCC1 in HEK293T cells to ascertain their associations as a second

screening. Among the listed proteins related to the ubiquitination/deubiquitination system, I could obtain or make expression constructs of 3xMyc-STUB1, 3xMyc-KCTD13, DCAF7-Myc, GFP-RNF220, 3xMyc-FBXO22, USP11-Myc, USP30-Myc, USP46-Myc, V5-TRIM28, 3xMyc-RNF40, 3xMyc-RNF2, MID1-Myc, GFP-CBL, FLAG-TRIM25, and FLAG-USP7. Those proteins were co-overexpressed with 3xFLAG-ERCC1 or non-tagged ERCC1 and co-immuprecipitated by various epitope-tag antibodies. As a result, 3xMyc-STUB1, 3xMyc-KCTD13, DCAF7-Myc, GFP-RNF220, 3xMyc-FBXO22, USP11-Myc, USP30-Myc and USP46-Myc were co-precipitated with ERCC1, while V5-TRIM28, 3xMyc-RNF40, 3xMyc-RNF2, MID1-Myc, GFP-CBL, FLAG-TRIM25 and FLAG-USP7 were not (Fig. 4).

Depletion of DCAF7 or USP11 affects the cellular levels of ERCC1-XPF.

Among the eight proteins that were verified to interact with ERCC1-XPF by immunoprecipitation experiments, I tested the impacts of siRNA-mediated knockdown of six interactors, DCAF7, STUB1, KCTD13, USP11, USP30 and USP46, on ERCC1-XPF protein level. As a result, I found that the knockdown of DCAF7 or USP11 in U2OS cells affects cellular level of ERCC1-XPF (Fig. 6), while the knockdown of other four interactors did not. In case of DCAF7 knockdown, the

cellular levels of both ERCC1 and XPF were markedly diminished. On the other hand, USP11 knockdown moderately reduced only ERCC1 level. These results suggest that DCAF7 and USP11 may play a regulatory role in controlling ERCC1-XPF level.

1-3. Discussion

In DNA maintenance systems, ERCC1-XPF is one of the most important factors which functions in not only NER but also other several DNA damage responses. ERCC1 and XPF need to form heterodimer to stabilize each other (Yagi et al., 1997; Jaspers et al., 2007; Tripsianes et al., 2005; Choi et al., 2005; Sanjeevani et al., 2010). ERCC1 was reported to interact with USP45 deubiquitinase, which appears to facilitate ERCC1 recruitment to DNA lesions rather than ERCC1 stability (Perez-Oliva et al., 2014). No other proteins involved in ubiquitination-mediated regulation of ERCC1-XPF were currently known.

For further understanding the function and regulation of ERCC1-XPF complex, I thought it is essential to identify novel interacting factors. In this study, I conducted tandem purification of double-tagged ERCC1 or XPF and mass spectrometry analysis, leading me to identify 699 candidate proteins. In particular, I have focused on 14 kinds of E3 ligases and five kinds of deubiquitinases included in the candidates. Verification process by co-immunoprecipitation experiments indicated that STUB1, KCTD13, DCAF7, RNF220, FBXO22, USP11, USP30 and USP46 appear truly positive as ERCC1-XPF interactors tested so far (Fig. 4).

STUB1 is known to interact with heat shock proteins, HSP70 and HSP90, and

ubiquitinate misfolded protein for their proteolytic degradation (Ballinger at al., 1999; Connel et al., 2001). STUB1 also ubiquitinates DNA Pol β involved in base excision repair (BER) and induces its degradation to regulate BER activity (Parsons et al., 2008). So STUB1 might also be involved in NER activity regulation by ubiquitinating ERCC1-XPF. KCDT13 is induced by TNF-α and interacts with PCNA and DNA Pol δ to activate DNA Pol δ (He et al., 2001). DCAF7, also known as WDR68 or HAN11, controls the cellular signaling as a scaffold protein or an adaptor protein and also functions as a substrate receptor of Cul4-DDB1 E3 ligase complex (see the Introduction section of Chapter 2). USP11 was reported to be deubiquitinase and stabilize p53 promoting DNA damage responses (Ke et al., 2014).

Knockdown experiments by siRNAs in selected six interactors revealed that DCAF7 and USP11 affect the steady state level of ERCC1-XPF (Fig. 6). Specially, the impact of DCAF7 was more prominent and ERCC1-XPF level was reduced to ~20%. I decided to focus on DCAF7 and at Chapter 2, the functional analysis of the interaction between DCAF7 and ERCC1-XPF was extensively analyzed.

Chapter 2 Functional analysis of one of the interacting proteins, DCAF7

2-1. Introduction

Background of DCAF7, a novel interacting protein with ERCC1-XPF

DDB1- and CUL4-associated factor 7 (DCAF7, also known as WDR68 or HAN11) is a WD40 domain which was discovered by a research of a kinase DYRK1A (dual-specificity tyrosine-phosphorylation regulated protein kinase/dual-specificity YAK1-related protein kinase) (Skurat and Dietrich, 2004). DCAF7 has five WD40 repeats. The N- and C-terminal have no manifest sequence similarity with the WD40 repeats. Because most of the structurally specified WD40 proteins contain seven WD40 repeats and form seven-bladed β-propeller structures (Stirnimann et al., 2010), it is speculated that DCAF7 has as least five β-propeller blades (Fig. 5A). Miyata et al., constructed a structural model of mammalian DCAF7 by analyzing its amino acid sequence (Miyata et al., 2014). DCAF7 is ecclesial for the proliferation and survival of mammalian cells (Ritterhoff et al., 2010; Miyata et al., 2011). DCAF7 can function as a substrate receptor of Cullin4-DDB1 complex and ubiquitinates target proteins, such as DNA ligase I and regulate their cellular levels (Peng et al., 2016). Since DCAF7 doesn't have nuclear localization signal, DCAF7

need to interact with DYRK1A which is a family of mammalian protein kinases (Miyata et al., 2011). DCAF7 is required for normal cellular levels of DYRK1A and DYRK1B (Yousefelahiyeh et al., 2018). DCAF7 works as a scaffold and mediates the interaction between kinases, DYRK1A, HIPK2 and MEKK (Glenewinkel et al., 2016; Ritterhoff et al., 2010). DCAF7 and DYRK1A form a complex and phosphorylates the C-terminal region of RNA polymesase II and promote myogenesis (Yu et al., 2019).

Molecular chaperon TRiC

In cells, newly synthesized proteins need to be properly folded. Molecular chaperones assist folding of many proteins. The chaperonin-containing T-complex (TRiC) is an ATP-dependent type II (group II) chaperon, prevents misfolding and aggregation during folding of many proteins (Hartle et al., 2002; Spiess et al., 2004; Horwich et al., 2007). TRiC consists of eight subunits (TCP1α to TCP1θ) (Fig. 5B) (Dunn et al., 2001). TRiC mainly recognizes exposed hydrophobic residues (Horwich et al., 2007), but charged animo acid residues can also be recognized (Spiess et al., 2006). It is reported that TRiC binds to DCAF7 and promotes its folding and nuclear localization (Miyata et al., 2014).

Functional analysis of DCAF7

Here at Chapter 2, I conducted several functional analysis to determine the mechanisms of DCAF7 against ERCC1-XPF. By co-immunoprecipitation analysis, I found out that DCAF7 interacts with XPF, not ERCC1. I further tried to determine the interacting region by partial XPF expression vectors. I speculate that DCAF7 interacts with XPF via not only one site but also multiple sites. The stabilization of ERCC1-XPF by DCAF7 was not depend on Cullin4-DDB1 complex. The reduction of ERCC1-XPF by depleted DCAF7 was not fully dependent on 26S proteasome, but some newly synthesized ERCC1 was partly dependent. Furthermore, I identified the molecular chaperon, TRiC as another regulator of the cellular levels of ERCC1-XPF. Importantly, DCAF7-depleted cells showed less efficient removal of UV-induced (6-4) photoproducts from the genome, indicating DCAF7 as a novel regulator of cellular NER.

2-2. Results

DCAF7 binds to ERCC1-XPF heterodimer through the association with XPF

I first tried to confirm the interaction between DCAF7 and ERCC1 or XPF by co-immunoprecipitation experiments with HEK293T cells transiently expressing epitope-tagged DCAF7 and ERCC1 (Figs. 7A) or XPF (Figs. 7B and C). In all types of combination, I could detect the co-immunoprecipitation between DCAF7 and ERCC1 or XPF, suggesting that DCAF7 indeed associates with ERCC1-XPF heterodimer in cells.

I next asked which subunit of the heterodimer interacts with DCAF7. For this purpose, instead of HEK293T cells, I used XP2YO(SV) cells from XP-F patient, in which mutant XPF protein is undetectable and the protein level of ERCC1 is marginal due to its destabilization (Matsumura et al., 1998). Interestingly, similar immunoprecipitation experiments exhibited co-precipitated DCAF7 and XPF (Figs. 8A and B), but not DCAF7 and ERCC1 (Figs. 8C and D). However, co-transfection of an increasing amount of XPF plasmid enabled us to detect ERCC1 coprecipitated with FLAG-DCAF7 by anti-FLAG antibody resin (Fig. 8E). These results strongly suggest that DCAF7 directly associates with XPF but indirectly with ERCC1.

XPF interacts with DCAF7 via multiple sites.

XPF consists of Helicase-like domain, nuclease domain and Helix-hairpin-helix motif, class 2. To identify which part of XPF is responsible for the DCAF7 binding, I made deletion mutants of Myc-tagged XPF (Fig. 9A) and examined their ability to interact with FLAG-tagged DCAF7 by co-immunoprecipitation analysis in XP2YO(SV) cells. Unexpectedly, both XPF (1-515)-Myc and XPF (516-916)-Myc which are not partially overlapped were co-immunoprecipitated with FLAG-DCAF7 (Fig. 9B and 9C). I assumed that the central part of XPF associates with DCAF7. Shorter region of C-terminus, XPF (719-916)-Myc was also co-immunoprecipitated in XP2YO(SV) (data not shown). Shorter region of N-terminus XPF (1-457)-Myc couldn't be overexpressed in XP2YO(SV) cells, but could be in HEK293T cells and also co-immunoprecipitated with FLAG-DCAF7 (data not shown). For these results, it is speculated that DCAF7 interact with XPF via multiple sites. DCAF7 might interact with their target proteins via several regions. I couldn't achieve any valuable functional insights from partial XPF and DCAF7 interaction analysis.

Depletion of DCAF7 reduces the cellular level of ERCC1-XPF.

To examine a functional role of DCAF7 and ERCC1-XPF interaction, U2OS

cells were transfected with DCAF7 siRNA (#1) and monitored for the cellular levels of XPF and ERCC1, in addition to DCAF7. Under the condition that DCAF7 was gradually decreased in a time-dependent manner, the protein levels of XPF and ERCC1 were also downregulated with similar kinetics (Fig. 10A). The DCAF7 depletion-induced ERCC1-XPF downregulation was reproducible (Fig. 10C), whereas the cellular levels of other NER factors (DDB1, DDB2 and XPB) were not affected by DCAF7 depletion (Fig. 10B). Moreover, I had a similar observation using HeLa cells with two different DCAF7 siRNAs, #1 and #2, targeting distinct regions of DCAF7 mRNA (Fig. 11A), indicating that this phenomenon is neither cell line-specific nor due to off-target effects.

The molecular chaperon TRiC, which plays an important role in proper folding of many proteins (Spiess et al., 2004; Horwich et al., 2007), has been reported to interact with DCAF7 and promote its folding and nuclear localization (Miyata et al., 2014). I examined the impact of depletion of TCP1α, one of eight subunits of TRiC, on the protein level of ERCC1-XPF. As shown in Fig. 10D, transfection of specific siRNA (#1) caused efficient TCP1α knockdown, but no change in DCAF7 protein level as reported previously (Miyata et al., 2014). The cellular level of ERCC1-XPF was also downregulated as expected, although no striking impacts on DDB2 and XPA

levels. Again, this phenomenon was reproducible (Fig. 10E) and was observed with another TCP1α siRNA sequence (#2) as well (Fig. 11B). Taken together, these results suggest that DCAF7 is required for maintaining the normal cellular levels of ERCC1-XPF.

DCAF7-mediated regulation of ERCC1-XPF level is independent of Cul4-DDB1 E3 ligase and 26S proteasome.

DCAF7 is known to form a complex with Cul4-DDB1 and to function as a substrate receptor that determines the substrate specificity of the E3 ligase complex. I wished to know whether the depletion of DDB1 also causes the downregulation of ERCC1-XPF. However, transfection of DDB1 siRNA affected neither the basal levels of ERCC1-XPF (Fig. 12A) nor the downregulation of ERCC1-XPF upon DCAF7 depletion (Fig. 12B), indicating that DDB1 and probably also Cul4 are unlikely to participate in this mechanism.

I further asked whether the downregulation of ERCC1-XPF by DCAF7 depletion is dependent on 26S proteasome. After transfection with DCAF7 siRNA, a proteasome inhibitor MG-132 was added to cell culture at 12 h and treated for 12 h before cell lysis. Immunoblot analysis showed that MG132 partially suppresses

the downregulation of ERCC1, while XPF level is unchanged (Fig. 12C). Non-ATPase regulatory subunit 14 (PSMD14), one of proteasome subunits, possesses a deubiquitinase activity and is essential for the proteolytic function of proteasome (Verma et al., 2002). Partial knockdown of PSMD14 by siRNA elevated basal levels of p53 and also DCAF7, XPF and ERCC1. Importantly, cotreatment of DCAF7 siRNA again caused the downregulation of ERCC1 and XPF (but not p53) (Fig. 12D), suggesting that the accumulation of ERCC1 and XPF by PSMD14 knockdown and their downregulation by DCAF7 knockdown are mutually independent.

Taken together, I suggest that the ubiquitin-proteasome system is not mainly implicated in DCAF7-mediated regulation of ERCC1-XPF level, although some fraction of ERCC1 regulation might be proteasome-dependent.

Depletion of DCAF7 causes the suppression of NER activity.

ERCC1-XPF is an indispensable factor for the dual incision reaction of NER. Given that DCAF7 depletion reduces the protein level of ERCC1-XPF, I wished to know the impact of DCAF7 depletion on cellular NER activity. To this end, I transfected HeLa cells with DCAF7 siRNA (#1) and measured the repair kinetics of 6-4PP induced by UV-C irradiation. DCAF7-depleted cells showed a significantly

slower rate of 6-4PP removal, compared to the undepleted control cells (Fig. 13A). I also performed the same experiment with Flp-In T-REx 293/FLAG-XPF-3xHis cells to check whether inducible expression of XPF can rescue the delay of 6-4PP repair. As seen in Fig. 13B, DCAF7 knockdown again suppressed 6-4PP repair, although less significantly compared with DCAF7-depleted HeLa cells, probably due to low knockdown efficiency in this cell line. Importantly, the treatment of doxycycline elevated the cellular level of exogenous FLAG-XPF-6xHis and even endogenous ERCC1, and restored the full 6-4PP repair ability. Taken together, these results suggest that DCAF7 plays an important role in maintaining normal NER activity by stabilizing ERCC1-XPF endonuclease.

DYRK1A kinase activity inhibitor, Harmine doesn't affect the cellular levels of ERCC1-XPF

There are several reports that DCAF7 acts as a scaffold of kinases and it is necessary for kinase pathways. Kinase DYRK1A interacts with DCAF7 and it is essential for the nuclear localization of DCAF7 (Miyata et al., 2011). DCAF7 is also required for normal cellular levels of DYRK1A and DYRK1B (Mina et al., 2018). The complex of DYRK1A and DCAF7 phosphorylates the C-terminal region of RNA

polymerase II and promote myogenesis (Dan et al., 2019). DCAF7 needs to serve a scaffold for kinases, HIPK2 and MEKK1 and their phosphorylation pathways (Stefanie et al., 2010). I speculate that DCAF7 acts as a scaffold protein and mediate the interaction between DYRK1A and XPF, and DYRK1A phosphorylates XPF to stabilize ERCC1-XPF. I used DYRK1A kinase activity inhibitor Harmine and analyzed its effects against ERCC1 and XPF levels (Figure 14). Even though the marker of kinase inhibition, Cyclin D1 levels were elevated (Chen et al., 2013), cellular levels of ERCC1 and XPF were not strikingly changed. DYRK1A kinase activity might not be involved in the mechanism of stabilization of ERCC1-XPF.

2-3. Discussion

In this study, I identified DCAF7 (also known as WDR68 or HAN11) as a novel interacting protein of ERCC1-XPF by a proteomic approach. Co-immunoprecipitation experiments confirmed their interaction and suggested a direct association of DCAF7 with XPF but not ERCC1, leading us to speculate an indirect interaction with ERCC1 probably via XPF.

Like most of WD40 proteins with seven WD40 repeats, DCAF7 forms a seven-bladed β-propeller structure, although it contains only five WD40 repeats (Miyata et al., 2014). One of known functions of DCAF7 is to control the cellular signaling as a scaffold protein of multiprotein complex or an adaptor protein recruiting downstream proteins by facilitating protein-protein interactions. DCAF7 binds to DYRK1A and DYRK1B belonging to the dual specificity tyrosine phosphorylation-regulated protein kinase (DYRK) family (Skurat and Dietrich, 2004; Nissen et al., 2006; Mazmanian et al., 2010; Miyata et al., 2011). DCAF7 also binds to MEKK1 and HIPK2, facilitating complex formation and signal transduction between the two protein kinases (Ritterhoff et al., 2010). Conversely, DYRK1A appears to contribute to the nuclear localization of DCAF7 through the physical interaction, independent of its kinase activity (Miyata et al., 2011).

Another known function of DCAF7 is as a substrate receptor of Cul4-DDB1 E3 ligase complex. The Cul4-DDB1 complex is a member of Cullin-RING finger E3 ligase family, which ubiquitinates target proteins (substrates) and mainly induces their proteasomal degradation. A large number of substrate receptors, DCAFs, have been identified (Lee and Zhou, 2007) and play an important role in determining the substrate specificity of the complex. DCAF7 was found to interact with DNA ligase I involved in DNA replication by joining Okazaki fragments, and to target it for ubiquitination by Cul4-DDB1 E3 ligase upon inhibition of cell proliferation (Peng et al., 2016).

Here, I found that DCAF7 depletion reduced the steady state level of ERCC1-XPF (Fig. 6) and hence the cellular NER activity (Fig. 13). The mechanism how DCAF7 stabilizes ERCC1-XPF is currently unknown, but several possible models can be proposed. First of all, the Cullin4-DDB1 complex is unlikely to participate in this mechanism, since knockdown of DDB1 influenced neither the basal level of ERCC1-XPF nor the downregulation of ERCC1-XPF upon DCAF7 depletion (Figs. 12A and B). On the other hand, Serine 256 of DCAF7 was recently reported to be a potential reactive site center of deubiquitination based on enhanced actively-based probes (ABPs) (Hewings et al., 2018). It is possible to speculate that the potential

deubiquitinase activity of DCAF7 might protect ERCC1-XPF from proteasomal degradation. However, it is currently unclear whether DCAF7 indeed possesses deubiquitinase activity.

A more plausible model would be that DCAF7 may function as an adopter protein to stabilize ERCC1-XPF. In fact, it was recently reported that DCAF7 is required for normal levels of DYRK1A and DYRK1B at a posttranslational level in a ubiquitin-proteasome-independent manner, although its detailed mechanism remains elusive (Yousefelahiyeh et al., 2018). In the context of this model, the molecular chaperone TRiC (TCP1 ring complex), also known as CCT (chaperonin containing TCP1), is possibly involved in DCAF7-mediated ERCC1-XPF stabilization. Nishida's group reported that TRiC binds to DCAF7 and promotes its folding, DYRK1A binding and nuclear accumulation (Miyata et al., 2014). Similarly, it has been also reported that TRiC binds to CSA, another DCAF protein with WD40 repeats, ensures its proper folding and complex formation with Cul4-DDB1 (Pines et al., 2018). It should be noted that, in our mass spectrometry analysis of ERCC1- or XPF-bound fraction, all of eight components of TRiC were detected (Table 2). I also obtained the result that TCP1 knockdown causes the downregulation of ERCC1-XPF level, as seen in DCAF7 knockdown (Figs. 10D and E), suggesting the possible

implication of TRiC in the DCAF7-mediated stabilization of ERCC1-XPF.

Another potential coplayer with DCAF7 may be protein kinase(s) that interacts with DCAF7. DCAF7 was reported to recruit DYRK1A and HIPK2 to the adenovirus E1A protein and mediate their interaction for phosphorylation (Glenewinkel et al., 2016). More recently, DCAF7 was found to stabilize and tether DYRK1A to RNA polymerase II, which promotes the hyperphosphorylation of its C-terminal domain (CTD) by DYRK1A and hence transcription of myogenic genes (Yu et al., 2019). In this model, some kinase(s) is possibly recruited to ERCC1-XPF complex or XPF before hetero-dimerization and facilitate the phosphorylation of XPF and/or ERCC1, thereby enhancing ERCC1-XPF stability. I need to test the possibility that protein kinases such as DYRK1A/B, HIPK2 and MEKK1 are also involved in the DCAF7-mediated ERCC1-XPF stabilization in near future.

In this study, I demonstrated that DCAF7, a novel interacting protein of ERCC1-XPF, plays some role in maintaining the cellular levels of ERCC1-XPF and nucleotide excision repair. As already mentioned, DCAF7 also functions in the negative regulation of the cellular level of DNA ligase I in quiescent cells, collectively suggesting that DCAF7 is one of key players controlling DNA metabolism. The cellular level of ERCC1-XPF is well known to influence the efficacy of platinum-

based cancer chemotherapy. This study provides a new insight into the regulatory mechanism of the cellular levels of ERCC1-XPF heterodimers and its application to anticancer therapy.

Materials and Methods

Cell lines and culture conditions

Parental Flp-In™ T-REx™ 293 (Invitrogen) and its derivative cell lines conditionally expressing FLAG-ERCC1-6xHis or FLAG-XPF-6xHis upon tetracycline or doxycycline treatment were grown in Dulbecco's modified Eagle medium (DMEM) (Gibco) supplemented with 10% fetal bovine serum (Sigma) and 10 μg/ml Penicillin-Streptomycin (Gibco). U2OS, HeLa and HEK293T cells were grown in DMEM (Wako) with 10% fetal bovine serum (Sigma) and 50 μg/ml Gentamicin (Nacalai tesque). All cell lines were cultured at 37°C in a humidified 5% CO_2 atmosphere.

Silver stain

The gel of SDS-PAGE is fixed by incubating with fix solution (50% MeOH, 12% Acetic Acid, 0.0185% HCHO) for one hour. The gel was washed with 50% ethanol for three times for 20 min each. The gel was pre-treated by incubating with pre-treat solution (0.02% sodium thiosulfate) for one minute, washed with water three times for 20 seconds each. The gel was impregnated by incubating with impregnate solution (12mM silver nitrate, 0.02775% HCHO) for 20 min, and washed twice by water for 20 seconds each. The gel was developed by incubated with develop solution (0.02%

sodium thiosulfate, 12% w/v $NaCO_3$) until bands of proteins become visible level, washed with water. The reaction was stopped by incubating with distain solution (12% acetic acid, 60% methanol, 1.2% glycerol).

Identification of ERCC1-XPF-interacting proteins by mass spectrometry

Flp-In™ T-REx™ 293 cell line (control) and Flp-In™ T-REx™ 293/FLAG-ERCC1-6xHis or FLAG-XPF-6xHis cell lines were incubated with 1 μg/ml tetracycline for 48 h to induce double-tagged bait proteins. Cell lysates were prepared in the lysis buffer (50 mM Tris-HCl, pH 7.4, 150 mM NaCl, 1 mM EDTA, 1% Triton X-100) containing EDTA-free protease inhibitor cocktail (Roche), supplemented with imidazole (final conc. 10 mM) (Sigma) and incubated with Ni-NTA agarose (Qiagen) for 1 h at 4°C. After washing with the lysis buffer containing 10 mM imidazole, bound fractions were eluted with the lysis buffer containing 200 mM imidazole. The eluates were incubated with anti-FLAG antibody agarose (Sigma) for 12 h at 4°C. The proteins bound to agarose were washed three times and eluted by incubating with the lysis buffer containing 150 μg/ml 3xFLAG peptide (Sigma) for 1 h at 4°C. The eluates were concentrated by chloroform-methanol extraction, dissolved in SDS sample buffer and fractionated by NuPAGE 10% Bis-Tris Protein Gels (Invitrogen).

The mass spectrometry analysis was conducted in the UNC Michael Hooker Proteomics Center.

Construction of expression vectors

A plasmid clone containing human DCAF7 cDNA was obtained from the Riken DNA bank (#HGX001752, Clone name: IRAK004G08). DCAF7 cDNA was subcloned into the pEF6/Myc-His vector (Thermo Fisher Scientific) using PCR with the primers, 5'-GTGGAATTCATGTCCCTGCACGGCAAACG (sense) and 5'-CGAGCGGCCGCCCACTCTGAGTATCTCCAGGC (antisense), or the pEF6-2xFLAG vector (Kind gift from Dr. Yamashita) by PCR with the primes, 5'-ATACATATGTCCCTGCACGGCAAACGGAA (sense) and 5'-CGAGCGGCCGCCTACACTCTGAGTATCTCCA (antisense). MID1 was also obtained from Riken DNA bank (Catalog#: HGX046310, Clone #: IRAK115M22) and Myc-tagged by subcloned into pEF6-Myc-His B. cDNAs of STUB1 (912, 11052 E08); KCTD13 (990, 11032 F11); RNF2 (1011, 11033 C01); FBXO22 (1212, 31006 F02) were obtained from Lineberger Tissue Culture Facility, hORFeome V5.1. and were inserted into the empty vector, pcDNA3-3Myc-DEST, which was kindly provided by Dr. Yue Xiong and 3xMyc-tagged by Gateway™ LR Clonase™ Enzyme mix (Thermo

Fisher Scientific) according to the manufacturer's instruction. TRIM25 (#12449), USP7 (#46751), USP11 (#22566), USP30 (#22578), USP46 (#22584) were obtained from Addgene. cDNAs of USP11, USP30, and USP46 are Myc-tagged by subcloned into pEF6-Myc-His B. GFP-RNF220 (pcDNA5-FRT/TO-GFP RNF220, DU Number: DU33230), GFP-CBL (pcDNA5-FRT/TO-GFP CBL, DU Number: DU31284) were obtained from MRC Protein Phosphorylation and Ubiquitylation Unit.

Immunoprecipitation

HEK 293T cells were transfected with various combinations of plasmids, pEF6/Myc-His, pEF6/DCAF7-Myc-His, pEF6/XPF-Myc-His, pEF6-2xFLAG, pEF6-2xFLAG-DCAF7, pEF6/3xFLAG-ERCC1, pcDNA3.1(+)/ERCC1 and pcDNA3.1(+)/XPF, and incubated for 48 h. Cell lysates were prepared with the NP-40 lysis buffer (50 mM Tris-Cl, pH 7.4, 150 mM NaCl, 1% Nonidet P-40) supplemented with EDTA-free protease inhibitor cocktail (Roche or Nacalai tesque), and incubated with anti-FLAG antibody resin (Wako) or anti-Myc antibody resin (Wako) for 1 h. After washing with the NP-40 lysis buffer three times, bound proteins were eluted by boiling with SDS sample buffer and analyzed by western blotting.

Antibodies and siRNA

The antibodies used in this study were as follows: anti-DCAF7 (EPR8712, Abcam), anti-ERCC1 (GTX129282, GeneTex), anti-TCP1α (sc-53454, Santa Cruz Biotechnology), anti-PSMD14 (A303-857A-T, Bethyl), anti-USP11 (A301-613A-T, Bethyl), anti-FLAG (PM020, MBL), anti-Myc (562, MBL). I also used home-made monoclonal antibodies against XPF (clone 19-16) and DDB1 (clone 43233-3-1) (Cosmo bio).

The siRNAs were obtained from Sigma-Aldrich: DCAF7 #1, 5'-GGAACAAGCAGGACCCUAAdTdT; DCAF7 #2, 5'-GGUGUUAGGGCGAGUGAAUdTdT. TCP1α #1, 5'-GACCAAAUUAGACAGAGAdTdT; TCP1α #2, 5'-GCAAGGAAGCAGUGCGUUAdTdT; PSMD14, 5'-GGCAUUAAUUCAUGGACUAdTdT. USP11, 5'-ACCGATTCTATTGGCCTAGTAdTdT. DDB1 siRNA was obtained from Cosmo Bio, 5'-GAAUUCAAUAAGGGCCUUdTdT. I also used siRNA Universal Negative Control #1 (Sigma) as control siRNA. U2OS or HeLa cells were transfected with siRNA using Lipofectamine™ RNAiMAX Transfection Reagent (Thermo Fisher Scientific) according to the manufacturer's instruction and incubated normally for

72 h.

Enzyme-linked immunosorbent assay (ELISA)

Cells grown in 35-mm dish were irradiated with 10 J/m^2 of UV-C from germicidal lamps (Toshiba, GL-10) and incubated for various periods. Genomic DNAs were isolated with the Geno Plus Genomic DNA Extraction Miniprep system (Viogene), and the amount of 6-4PP was measured by using 64M-5 antibody as described previously (Mori et al., 1991).

ACKNOWLEDGEMENTS

The first half of this study was carried out by the support of Tobitate! (Leap for Tomorrow) Study Abroad Initiative. Thanks to the scholarship, I could achieve a precious opportunity to visit the University of North Carolina at Chapel Hill to study. I'd like to thank all people who are working for the scholarship, including Ministry of Education, Culture, Sports, Science and Technology, and supporting companies.

I would like to express my deepest gratitude to Dr. Aziz Sancar for giving me a great opportunity to study at his laboratory and a lot of supports. His comments and suggestions were innumerably valuable. I was also helped by members of Dr. Sancar's laboratory, Dr. Laura Lindsey-Boltz, Dr. Christpher Selby, Dr. Michael Kemp, Dr. Yi-Ying Chiou, Dr. Jinchuan Hu, Dr. Yangyan Yang, Dr. Wentao Li, Dr. Sheera Adar, Dr. Fazile Canturk, Dr. Muhammet Karaman, Dr. Wentao Li, Dr. Gulnihal Kulaksiz. I employed the Flp-In T-REx 293 cells which were constructed by Dr. Joyce Reardon. To conduct mass spectrometry analysis, Laura Herring gave me a lot of advices. I got a support from Dr. Yue Xiong's laboratory for proteomics analysis of uniquitination and Dr. Naoya Sasaki directed me how to proceed the research.

Also, I would like to thank Professor Tsukasa Matsunaga for his constant devoting

attitude towards me, not only for my research but also my health, future careers, and financial conditions. I also thank Dr. Mitsuo Wakasugi for appropriate guides, comments for proceeding my research, and improvement of my journal. Dr. Katsumi Yamashita kindly gave me a plasmid and a lot of supportive advices. Daily I communicate and share a lot of data, tips, and opinions with Ryo Akahori. He gave me a plasmid he made. I strongly hope that he will continue this research and determine further molecular mechanisms of cellular level and localization of the heterodimer, ERCC1-XPF. Additionally, I've been supported by all of other members of the Human Molecular Genetics laboratory. My family gave me a valuable opportunity to study at the lab, and gave me a lot of supports. Many people helped me with my mental conditions. I'd like to thank all of those people who have been supporting me.

This research is based in part upon work conducted using the UNC Michael Hooker Proteomics Center, which is supported in part by the NIH-NCI Grant No. CA016086 to the Lineberger Comprehensive Cancer Center.

References

Adair, G. M., Rolig, R. L., Moore-Faver, D., Zabelshansky, M., Wilson, J. H., Nairn, R. S. (2000) Role of ERCC1 in removal of long non-homologous tails during targeted homologous recombination. The EMBO J. 19, 5552–5561.

Adebali, O., Chiou, Y. Y., Hu, J., Sancar, A., Selby CP. (2017a) Genome-wide transcription-coupled repair in Escherichia coli is mediated by the Mfd translocase. Proc Natl Acad Sci U S A. 114, E2116–E2125.

Adebali. O., Sancar, A., Selby, C. P. (2017b) Mfd translocase is necessary and sufficient for transcription-coupled repair in Escherichia coli. J Biol Chem. 292, 18386-18391.

Ahmad, A., Robinson, A. R., Duensing, A., van Drunen, E., Beverloo, H. B., Weisberg, D. B., Hasty, P., Hoeijmakers, J. H., Niedernhofer, L. J. (2008) ERCC1-XPF endonuclease facilitates DNA double-strand break repair. Mol Cell Biol. 28, 5082–5092.

Al-Minawi, A. Z., Saleh-Gohari, N., Helleday, T. (2008) The ERCC1/XPF endonuclease is required for efficient single-strand annealing and gene conversion in mammalian cells. Nucleic Acids Res 36, 1–9.

Araújo, S. J., Tirode, F., Coin, F., Pospiech, H., Syväoja, J. E., Stucki, M., Hübscher, U., Egly, J. M., Wood, R. D. (2000) Nucleotide excision repair of DNA with recombinant human proteins: definition of the minimal set of factors, active forms of TFIIH, and modulation by CAK. Genes Dev. 14, 349–359.

Arora, S., Kothandapani, A., Tillison, K., Kalman-Maltese, V., Patrick. S. M. (2010) Downregulation of XPF-ERCC1 enhances cisplatin efficacy in cancer cells. DNA Repair 9, 745–753.

Ballinger, C. A., Connell, P., Wu, Y., Hu, Z., Thompson, L. J., Yin, L. Y., Patterson, C. (1999) Identification of CHIP, a novel tetratricopeptide repeat-containing protein that interacts with heat shock proteins and negatively regulates chaperone functions. Mol Cell Biol. 19, 4535–4545.

Bennardo, N., Cheng, A., Huang, N., Stark, J. M. (2008) Alternative-NHEJ is a mechanistically distinct pathway of mammalian chromosome break repair. PLoS genetics 4, e1000110.

Biggerstaff, M., Szymkowski, D. E., Wood, R. D. (1993) Co-correction of the ERCC1, ERCC4 and xeroderma pigmentosum group F DNA repair defects in vitro. The EMBO J. 12, 3685–3692.

Bouwman, P, Jonkers, J. (2012) The effects of deregulated DNA damage signalling on cancer chemotherapy response and resistance. Nat Rev Cancer. 12, 587–598.

Chen, J. Y., Lin, J. R., Tsai, F. C., Meyer, T. (2014) Dosage of Dyrk1a shifts cells within a p21-cyclin D1 signaling map to control the decision to enter the cell cycle. Mol Cell. 52, 87–100.

Choi, Y. J., Ryu, K. S., Ko, Y. M., Chae, Y. K., Pelton, J. G., Wemmer, D. E., Choi, B. S. (2005) Biophysical characterization of the interaction domains and mapping of the contact residues in the XPF-ERCC1 complex. J Biol Chem. 280, 28644–28652.

Cleaver, J. E., Lam, E. T., Revet, I. (2009) Disorders of nucleotide excision repair: the genetic and molecular basis of heterogeneity. Nat Rev Genet. 10, 756–768.

Connell, P., Ballinger, C. A., Jiang, J., Wu, Y., Thompson, L. J., Höhfeld, J., Patterson, C. (2001) The co-chaperone CHIP regulates protein triage decisions mediated by heat-shock proteins. Nat Cell Biol. 3, 93–96.

de Laat W. L., Sijbers, A. M., Odijk, H., Jaspers, N. G., Hoeijmakers, J. H. (1998b) Mapping of interaction domains between human repair proteins ERCC1 and XPF. Nucleic Acids Res. 26, 4146–4152.

de Laat, W. L., Appeldoorn, E., Sugasawa, K., Weterings, E., Jaspers, N. G., Hoeijmakers, J. H. (1998) DNA-binding polarity of human replication protein A positions nucleases in nucleotide excision repair. Genes Dev. 12, 2598–609.

de Laat, W.L., Appeldoorn, E., Jaspers, N. G., Hoeijmakers, J. H. (1998a) DNA structural elements required for ERCC1-XPF endonuclease activity. J Biol Chem. 273, 7835–7842.

De Silva, I. U., McHugh, P. J., Clingen, P. H., Hartley, J. A. (2000) Defining the roles of nucleotide excision repair and recombination in the repair of DNA interstrand cross-links in mammalian cells. Mol Cell Biol 20, 7980–7990.

De Silva, I. U., McHugh, P. J., Clingen, P. H., Hartley, J. A. (2002) Defects in interstrand cross-link uncoupling do not account for the extreme sensitivity of ERCC1 and XPF cells to cisplatin. Nucleic Acids Res. 30, 3848–3856.

Dunn, A. Y., Melville, M. W., Frydman, J. (2001) Review: cellular substrates of the eukaryotic chaperonin TRiC/CCT. J Struct Biol. 135, 176–184.

Enzlin, J. H., Schärer, O. D. (2002) The active site of the DNA repair endonuclease XPF-ERCC1 forms a highly conserved nuclease motif. EMBO J. 21, 2045–2053.

Fisher, L. A., Bessho, M., Bessho, T. (2008) Processing of a psoralen DNA interstrand cross-link by XPF-ERCC1 complex in vitro. J Biol Chem. 283, 1275–1281.

Friedberg, E. C., Aguilera, A., Gellert, M., Hanawalt, P. C., Hays, J. B., Lehmann, A.R., Lindahl, T., Lowndes, N., Sarasin, A., Wood, R. D. (2006) DNA repair: from molecular mechanism to human disease. DNA Repair 5, 986–996.

Friedberg, E. C., Walker, G. C., Siede, W., Wood, R. D., Schultz, R. A. Ellenberger, T. (2006) DNA Repair and Mutagenesis. 2nd Edition, ASM Press, Washington DC.

Glenewinkel, F., Cohen, M. J., King, C. R., Kaspar, S., Bamberg-Lemper, S., Mymryk, J. S., Becker, W. (2016) The adaptor protein DCAF7 mediates the interaction of the adenovirus E1A oncoprotein with the protein kinases DYRK1A and HIPK2. Sci Rep. 6, 28241.

Gregg, S. Q., Robinson, A. R., and Niedernhofer, L. J. (2011) Physiological consequences of defects in ERCC1-XPF DNA repair endonuclease. DNA Repair 10, 781–791.

Hartl, F. U., Hayer-Hartl, M. (2002) Molecular chaperones in the cytosol: from nascent chain to folded protein. Science 295, 1852–1858.

He, H., Tan, C. K., Downey, K. M., So, A. G. (2001) A tumor necrosis factor alpha- and interleukin 6-inducible protein that interacts with the small subunit of DNA polymerase

delta and proliferating cell nuclear antigen. Proc Natl Acad Sci U S A. 98, 11979–11984.

Hewings, D. S., Heideker, J., Ma, T. P., AhYoung, A. P., El Oualid, F., Amore, A., Costakes, G. T., Kirchhofer, D., Brasher, B., Pillow, T., Popovych, N., Maurer, T., Schwerdtfeger, C., Forrest, W. F., Yu, K., Flygare, J., Bogyo, M., Wertz, I. E., (2018) Reactive-site-centric chemoproteomics identifies a distinct class of deubiquitinase enzymes. Nat Commun. 9, 1162.

Horwich, A. L., Fenton, W. A., Chapman, E., Farr, G. W. (2007) Two families of chaperonin: physiology and mechanism. Annu Rev Cell Dev Biol. 23, 115–145.

Horwich, A. L., Fenton, W. A., Chapman, E., Farr, G. W. (2007) Two families of chaperonin: physiology and mechanism. Annu. Rev. Cell Dev. Biol. 23, 115–145.
Hu, J., Selby, C. P., Adar, S., Adebali, O., Sancar, A. (2017) Molecular mechanisms and genomic maps of DNA excision repair in Escherichia coli and humans. J Biol Chem. 292, 15588–15597.

Jaspers, N. G., Raams, A., Silengo, M. C., Wijgers, N., Niedernhofer, L. J., Robinson, A. R., Giglia-Mari, G., Hoogstraten, D., Kleijer, W. J., Hoeijmakers, J. H., Vermeulen, W. (2007) First reported patient with human ERCC1 deficiency has cerebro-oculo-facio-skeletal syndrome with a mild defect in nucleotide excision repair and severe developmental failure. Am J Hum Genet. 80, 457–466.

Kashiyama, K., Nakazawa, Y., Pilz, D. T., Guo, C., Shimada, M., Sasaki, K., Fawcett, H., Wing, J. F., Lewin, S. O., Carr, L., Li, T. S., Yoshiura, K., Utani, A., Hirano, A., Yamashita, S., Greenblatt, D., Nardo, T., Stefanini, M., McGibbon, D., Sarkany, R., Fassihi, H., Takahashi, Y., Nagayama, Y., Mitsutake, N., Lehmann, A. R., Ogi, T. (2013) Malfunction of nuclease ERCC1-XPF results in diverse clinical manifestations and causes Cockayne syndrome, xeroderma pigmentosum, and Fanconi anemia. Am J Hum Genet. 92, 807–19.

Ke, J. Y., Dai, C. J., Wu, W. L., Gao, J. H., Xia, A. J., Liu, G. P., Lv, K. S., Wu, C. L. (2014) USP11 regulates p53 stability by deubiquitinating p53. J Zhejiang Univ Sci B. 15, 1032–1038.

Klein, Douwel, D., Boonen, R. A., Long, D. T., Szypowska, A. A., Raschle, M., Walter, J.C., Knipscheer, P. (2014) XPF-ERCC1 acts in Unhooking DNA interstrand crosslinks in cooperation with FANCD2 and FANCP/SLX4. Mol Cell 54, 460–471.

Kuraoka, I., Kobertz, W. R., Ariza, R. R., Biggerstaff, M., Essigmann, J. M., Wood, R. D. (2000) Repair of an interstrand DNA cross-link initiated by ERCC1-XPF repair/recombination nuclease. J Biol Chem. 275, 26632–26636.

Lan, L., Hayashi, T., Rabeya, R. M., Nakajima, S., Kanno, Si, Takao, M., Matsunaga, T., Yoshino, M., Ichikawa, M., Riele, Ht, Tsuchiya, S., Tanaka, K., Yasui, A. (2004) Functional and physical interactions between ERCC1 and MSH2 complexes for resistance to cis-diamminedichloroplatinum(II) in mammalian cells. DNA Repair 3, 135–143.

Lee, J., Zhou, P. (2007) DCAFs, the missing link of the CUL4-DDB1 ubiquitin ligase. Mol Cell. 26, 775–780.

Li, W., Adebali, O., Yang, Y., Selby, C. P., Sancar, A. (2018) Single-nucleotide resolution dynamic repair maps of UV damage in Saccharomyces cerevisiae genome. Proc Natl Acad Sci U S A. 115, E3408–E3415.

Manandhar, M., Boulware, K. S., Wood, R. D. (2015) The ERCC1 and ERCC4 (XPF) genes and gene products. Gene 569, 153–161.

Matsumura, Y., Nishigori, C., Yagi, T., Imamura, S., Takebe, H. (1998) Characterization of molecular defects in xeroderma pigmentosum group F in relation to its clinically mild symptoms. Hum Mol Genet. 7, 969–974.

Matsunaga, T., Park, C. H., Bessho, T., Mu, D., Sancar, A. (1996) Replication protein A confers structure-specific endonuclease activities to the XPF-ERCC1 and XPG subunits of human DNA repair excision nuclease. J Biol Chem. 271, 11047–11050.

Mazmanian G, Kovshilovsky M, Yen D, Mohanty A, Mohanty S, Nee A, Nissen RM. (2010) The zebrafish dyrk1b gene is important for endoderm formation. Genesis. 48, 20–30.

McWhir, J., Selfridge, J., Harrison, D. J., Squires, S., Melton, D. W. (1993) Mice with DNA repair gene (ERCC-1) deficiency have elevated levels of p53, liver nuclear abnormalities and die before weaning. Nat Genet. 5, 217–224.

Miyata, Y., Nishida, E. (2011) DYRK1A binds to an evolutionarily conserved WD40-repeat protein WDR68 and induces its nuclear translocation. Biochim Biophys Acta. 1813, 1728–1739.

Miyata, Y., Shibata, T., Aoshima, M., Tsubata, T., Nishida, E. (2014) The molecular chaperone TRiC/CCT binds to the Trp-Asp 40 (WD40) repeat protein WDR68 and promotes its folding, protein kinase DYRK1A binding, and nuclear accumulation. J Biol Chem. 289, 33320–33332.

Muñoz, I. M., Hain, K., Déclais, A. C., Gardiner, M., Toh, G. W., Sanchez-Pulido, L., Heuckmann, J. M., Toth, R., Macartney, T., Eppink, B., Kanaar, R., Ponting, C. P., Lilley, D. M., Rouse, J. (2009) Coordination of structure-specific nucleases by human SLX4/BTBD12 is required for DNA repair. Mol Cell. 35, 116–127.

Muñoz, P., Blanco, R., Flores, J. M., Blasco, M. A. (2005) XPF nuclease-dependent telomere loss and increased DNA damage in mice overexpressing TRF2 result in premature aging and cancer. Nat Genet. 37, 1063–1071.

Niedernhofer, L. J., Garinis, G. A., Raams, A., Lalai, A. S., Robinson, A. R., Appeldoorn, E., Odijk, H., Oostendorp, R., Ahmad, A., van Leeuwen, W., Theil, A. F., Vermeulen, W., van der Horst, G. T., Meinecke, P., Kleijer, W. J., Vijg, J., Jaspers, N. G., Hoeijmakers, J. H. (2006) A new progeroid syndrome reveals that genotoxic stress suppresses the somatotroph axis. Nature 444, 1038–1043.

Niedernhofer, L. J., Odijk, H., Budzowska, M., van Drunen, E., Maas, A., Theil, A. F., de Wit, J., Jaspers, N. G., Beverloo, H. B., Hoeijmakers, J. H., Kanaar, R. (2004) The structure-specific endonuclease Ercc1-Xpf is required to resolve DNA interstrand cross-link-induced double-strand breaks. Mol Cell Biol. 24, 5776–5787.

Nissen, R. M., Amsterdam, A., Hopkins, N. (2006) A zebrafish screen for craniofacial mutants identifies wdr68 as a highly conserved gene required for endothelin-1 expression. BMC Dev Biol. 7, 28.

Núñez, F., Chipchase, M. D., Clarke, A. R., Melton, D. W. (2000) Nucleotide excision repair gene (ERCC1) deficiency causes G2 arrest in hepatocytes and a reduction in liver binucleation: the role of p53 and p21. FASEB J. 14, 1073–1082.

Park, C. H., Sancar, A. (1994) Formation of a ternary complex by human XPA, ERCC1, and ERCC4 (XPF) excision repair proteins. Proc Natl Acad Sci U S A. 91, 5017–5021.
Parsons, J. L., Tait, P. S., Finch, D., Dianova, I. I., Allinson, S. L., Dianov, G. L. (2008) CHIP-mediated degradation and DNA damage-dependent stabilization regulate base excision repair proteins. Mol Cell. 29, 477–487.

Peng, Z., Liao, Z., Matsumoto, Y., Yang, A., Tomkinson, A. E. (2016) Human DNA Ligase I Interacts with and Is Targeted for Degradation by the DCAF7 Specificity Factor of the Cul4-DDB1 Ubiquitin Ligase Complex. J Biol Chem. 291, 21893–21902.

Perez-Oliva, A. B., Lachaud, C., Szyniarowski, P., Muñoz, I., Macartney, T., Hickson, I., Rouse, J., Alessi, D. R. (2015) deubiquitylase controls ERCC1-XPF endonuclease-mediated DNA damage responses. EMBO J. 34, 326–343.

Pines, A., Dijk, M., Makowski, M., Meulenbroek, E. M., Vrouwe, M. G., van der Weegen, Y., Baltissen, M., French, P. J., van Royen, M. E., Luijsterburg, M. S., Mullenders, L. H., Vermeulen, M., Vermeulen, W., Pannu, N. S., van Attikum, H. (2018) TRiC controls transcription resumption after UV damage by regulating Cockayne syndrome protein A. Nat Commun. 9, 1040.

Reardon, J. T., Thompson, L. H., Sancar, A. (1993) Excision repair in man and the molecular basis of xeroderma pigmentosum syndrome. Cold Spring Harb Symp Quant Biol. 58, 605–617.

Ritterhoff, S., Farah, C. M., Grabitzki, J., Lochnit, G., Skurat, A. V., Schmitz, M. L. (2010) The WD40-repeat protein Han11 functions as a scaffold protein to control HIPK2 and MEKK1 kinase functions. EMBO J. 29, 3750–3761.

Sargent, R. G., Rolig, R. L., Kilburn, A. E., Adair, G. M., Wilson, J. H., Nairn, R. S. (1997) Recombination-dependent deletion formation in mammalian cells deficient in the nucleotide excision repair gene ERCC1. Proc Natl Acad Sci U S A. 94, 13122–13127.

Schärer, O. D. (2013) Nucleotide excision repair in eukaryotes. Cold Spring Harb Perspect Biol. 5, a012609.

Sijbers, A. M., de Laat, W. L., Ariza, R. R., Biggerstaff, M., Wei, Y. F., Moggs, J. G., Carter, K. C., Shell, B. K., Evans, E, de Jong M. C., Rademakers, S., de Rooij, J., Jaspers, N. G.,

Hoeijmakers, J. H., Wood, R. D. (1996) Xeroderma pigmentosum group F caused by a defect in a structure-specific DNA repair endonuclease. Cell. 86, 811–822.

Skurat, A. V., Dietrich, A.D. (2004) Phosphorylation of Ser640 in muscle glycogen synthase by DYRK family protein kinases. J Biol Chem. 279, 2490–2498.

Spiess, C., Meyer, A. S., Reissmann, S., Frydman, J. (2004) Mechanism of the eukaryotic chaperonin: protein folding in the chamber of secrets. Trends Cell Biol. 14, 598–604.

Spiess, C., Miller, E. J., McClellan, A. J., Frydman, J. (2006) Identification of the TRiC/CCT substrate binding sites uncovers the function of subunit diversity in eukaryotic chaperonins. Mol Cell. 24, 25–37.

Stirnimann, C. U., Petsalaki, E., Russell, R. B., Müller, C. W. (2010) WD40 proteins propel cellular networks. Trends Biochem Sci. 35, 565–574.

Tripsianes, K., Folkers, G., Ab, E., Das, D., Odijk, H., Jaspers, N. G., Hoeijmakers, J. H., Kaptein, R., Boelens, R. (2005) The structure of the human ERCC1/XPF interaction domains reveals a complementary role for the two proteins in nucleotide excision repair. Structure 13, 1849–1858.

van Vuuren, A. J., Appeldoorn, E., Odijk, H., Yasui, A., Jaspers, N. G., Bootsma, D., Hoeijmakers, J. H. (1993) Evidence for a repair enzyme complex involving ERCC1 and complementing activities of ERCC4, ERCC11 and xeroderma pigmentosum group F. EMBO J. 12, 3693–3701.

Verma, R., Aravind, L., Oania, R., McDonald, W. H., Yates, J. R. 3rd ., Koonin, E. V., Deshaies, R. J. (2002) Role of Rpn11 metalloprotease in deubiquitination and degradation by the 26S proteasome. Science. 298, 611–615.

Wan, B., Yin, J., Horvath, K., Sarkar, J., Chen, Y., Wu, J., Wan, K., Lu, J., Gu, P., Yu, E. Y., Lue, N. F., Chang, S., Liu, Y., Lei, M. (2013) SLX4 assembles a telomere maintenance toolkit by bridging multiple endonucleases with telomeres. Cell Rep. 4, 861–869.

Weeda, G., Donker, I., de Wit, J., Morreau, H., Janssens, R., Vissers, C. J., Nigg, A., van Steeg, H., Bootsma, D., Hoeijmakers, J. H. (1997) Disruption of mouse ERCC1 results in a novel repair syndrome with growth failure, nuclear abnormalities and senescence.

Curr Biol. 7, 427–439.

Wu, Y., Mitchell, T. R., Zhu, X. D. (2008) Human XPF controls TRF2 and telomere length maintenance through distinctive mechanisms. Mech Ageing 129, 602–610.

Yagi, T., Wood, R. D., Takebe, H. (1997) A low content of ERCC1 and a 120 kDa protein is a frequent feature of group F xeroderma pigmentosum fibroblast cells. Mutagenesis. 12, 41–44.

Yousefelahiyeh, M., Xu, J., Alvarado, E., Yu, Y., Salven, D., Nissen, R. M. (2018) DCAF7/WDR68 is required for normal levels of DYRK1A and DYRK1B. PLoS One 13, e0207779.

Yu, D., Cattoglio, C., Xue, Y., Zhou, Q. (2019) A complex between DYRK1A and DCAF7 phosphorylates the C-terminal domain of RNA polymerase II to promote myogenesis. Nucleic Acids Res. 47, 4462–4475.

Zhu, X. D., Niedernhofer, L., Kuster, B., Mann, M., Hoeijmakers, J. H., de Lange, T. (2003) ERCC1/XPF removes the 3' overhang from uncapped telomeres and represses formation of telomeric DNA-containing double minute chromosomes. Mol Cell. 12, 1489–1498.

Table

Protein	Symbol	No. of peptides in ERCC1 fraction	No. of peptides in XPF fraction
DDB1- and CUL4-associated factor 7	DCAF7	11	7
E3 ubiquitin-protein ligase CHIP	STUB1	9	10
Transcription intermediary factor 1-beta	TRIM28	13	6
E3 ubiquitin-protein ligase BRE1B	RNF40	6	7
E3 ubiquitin-protein ligase BRE1A	RNF20	10	3
F-box only protein 21	FBXO21	5	0
E3 ubiquitin-protein ligase Midline-1	MID1	6	1
E3 ubiquitin-protein ligase RING2	RNF2	2	0
BTB/POZ domain-containing adapter for CUL3-mediated RhoA degradation protein 1	KCTD13	2	0
E3 ubiquitin/ISG15 ligase TRIM25	TRIM25	4	0
F-box only protein 22	FBXO22	2	0
E3 ubiquitin-protein ligase TRIM38	TRIM38	2	0
E3 ubiquitin-protein ligase CBL	CBL	2	1
E3 ubiquitin-protein ligase RNF220	RNF220	2	0
Ubiquitin carboxyl-terminal hydrolase 7	USP7	14	12
Ubiquitin carboxyl-terminal hydrolase 30	USP30	2	0
Ubiquitin carboxyl-terminal hydrolase 46	USP46	2	0
Ubiquitin carboxyl-terminal hydrolase 11	USP11	2	3
Probable ubiquitin carboxyl-terminal hydrolase FAF-X	USP9X	4	0
DNA repair protein complementing XP-A cells	XPA	5	1
DNA mismatch repair protein Msh2	MSH2	1	3
Structure-specific endonuclease subunit SLX4	SLX4	3	1

Table 1. Proteomic analysis data on E3 ligases and deubiquitinases.
The numbers of peptides from 14 kinds of E3 ligases and 5 kinds of deubiquitinases detected in mass spectrometry are listed. Data on XPA, MSH2 and SLX4, well-known interactors of ERCC1-XPF was also shown.

Protein	Symbol	No. of peptides in ERCC1 fraction	No. of peptides in XPF fraction
T-complex protein 1 subunit alpha	TCP1	16	10
T-complex protein 1 subunit beta	CCT2	16	9
T-complex protein 1 subunit gamma	CCT3	9	4
T-complex protein 1 subunit delta	CCT4	9	3
T-complex protein 1 subunit epsilon	CCT5	5	1
T-complex protein 1 subunit zeta	CCT6A	2	2
T-complex protein 1 subunit eta	CCT7	9	0
T-complex protein 1 subunit theta	CCT8	11	4

Table 2. Proteomic analysis data on TRiC/CCT components
All eight components of TRiC/CCT were detected in mass spectrometry and the numbers of peptides from each component are listed.

Figure

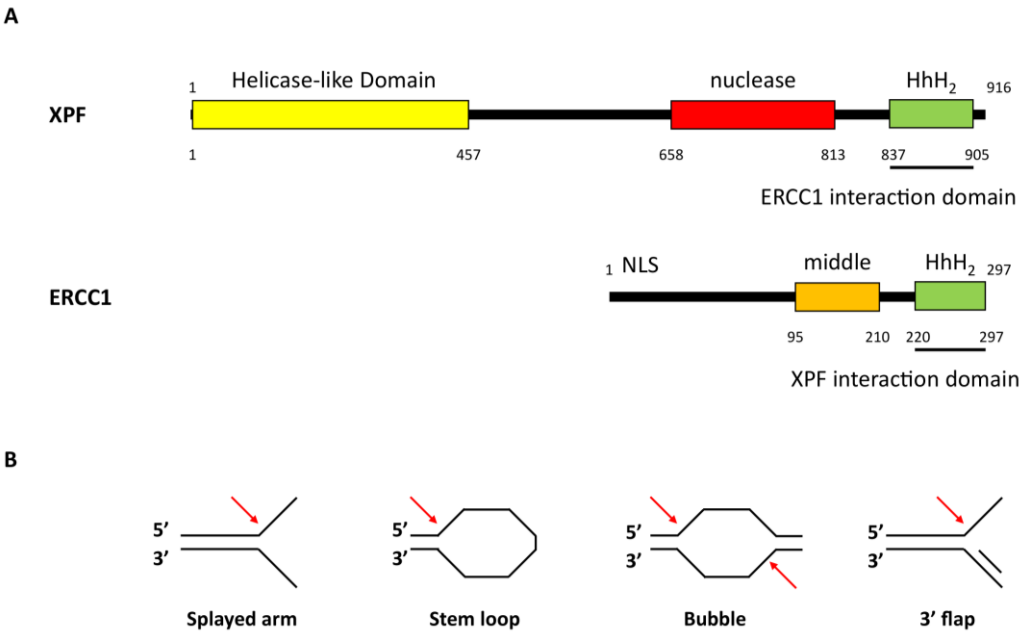

Figure 1. Structure and functions of ERCC1-XPF
(A) Schematic representation of various domains and known interaction regions of XPF and ERCC1.
(B) Schematic representation of the structures of DNA substrates for ERCC1-XPF endonuclease.

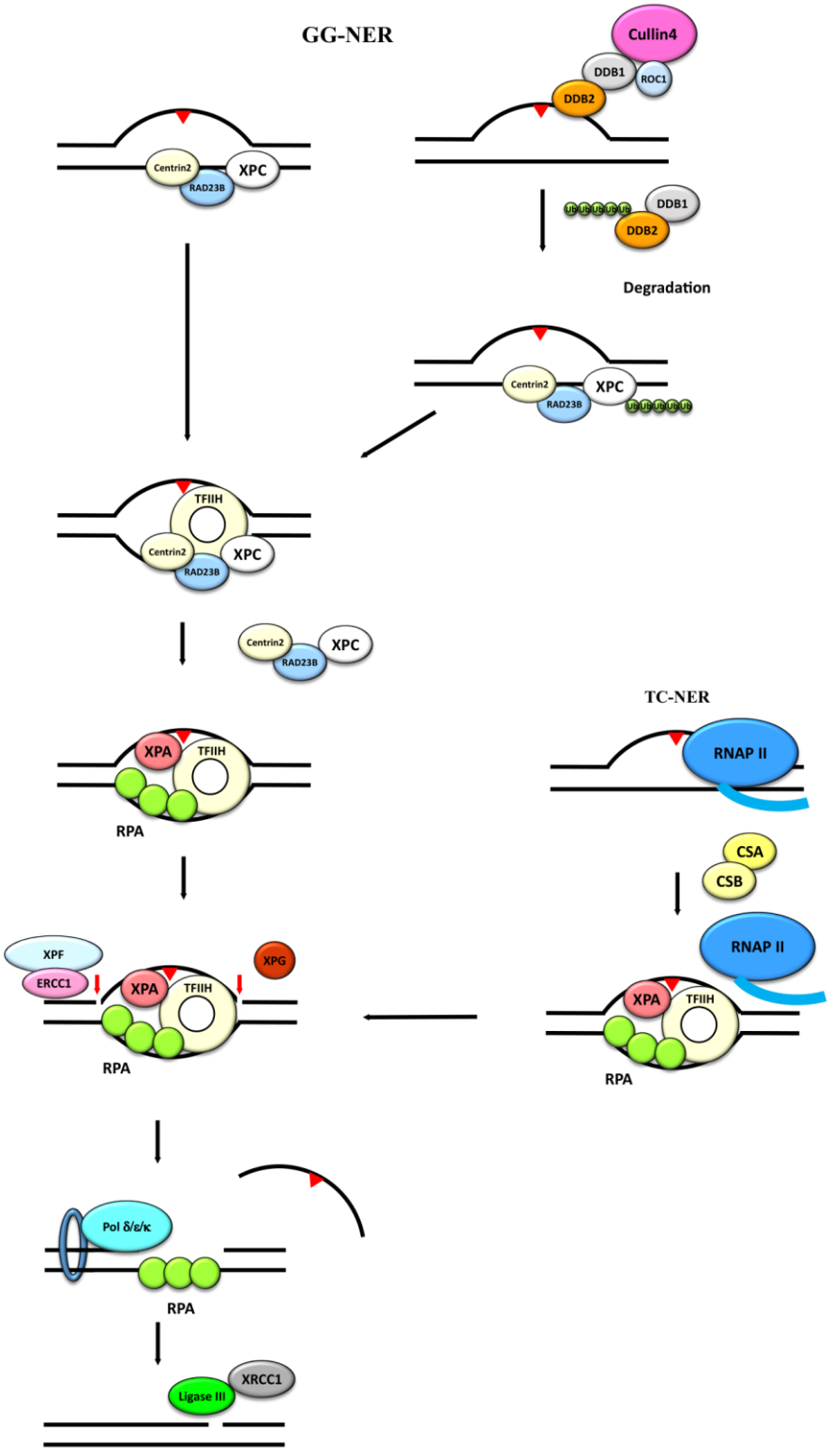

Figure. 2　Outline of Nucleotide excision repair core reaction

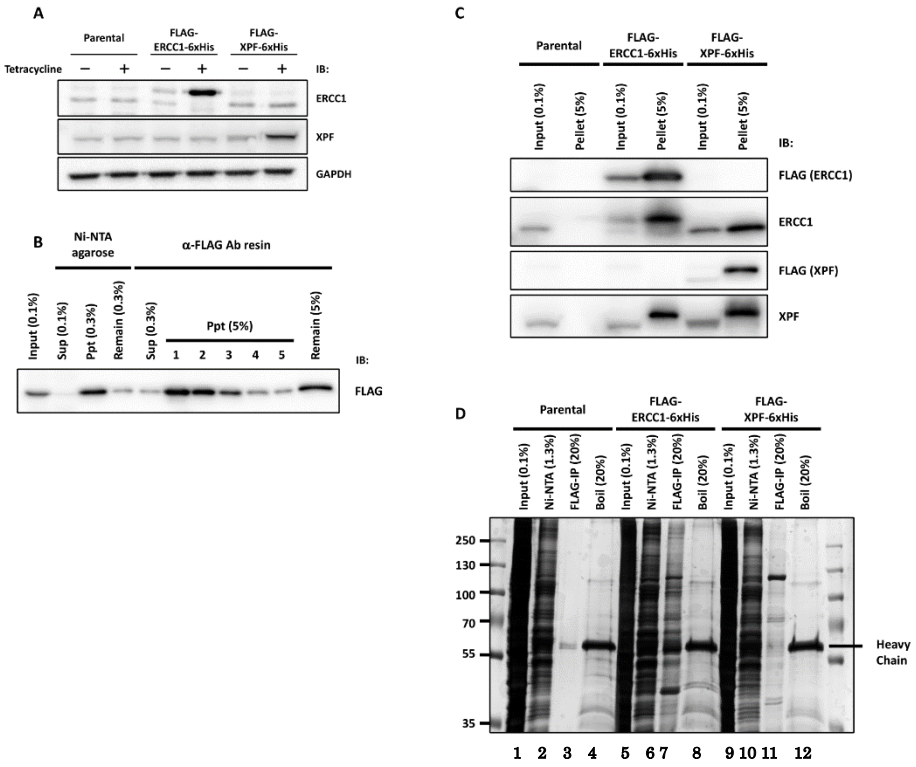

Figure. 3 Overexpression of ERCC1 or XPF in Flp-In TREx 293 cells and tandem affinity purification.
(A) Parental Flp-In™ T-REx™ 293 and its derivative cell lines conditionally expressing FLAG-ERCC1-6xHis or FLAG-XPF-6xHis were treated with or without 1 μg/mL tetracycline for 48 h and lysed. Each cell lysate was analyzed by western blotting with the indicated antibodies. (B) Cell lysate from tetracycline-treated Flp-In T-REx 293 /FLAG-ERCC1-6xHis cells was incubated with Ni-NTA agarose and subsequently with anti-FLAG antibody resin. Bound proteins were eluted with 3xFLAG peptides five times and remaining proteins bound to the resin were eluted by boiling with SDS sample buffer. Aliquots of samples from each step were separated on SDS-PAGE and analyzed by western blotting with anti-FLAG antibody. (C) Cell lysates from the three cell lines were processed for tandem purification as described in (B), and the lysates (Input) and the precipitates (Pellet) were analyzed by western blotting with the indicated antibodies. (D) Each fraction of tandem purification steps was separated on SDS-PAGE and visualized by silver staining.

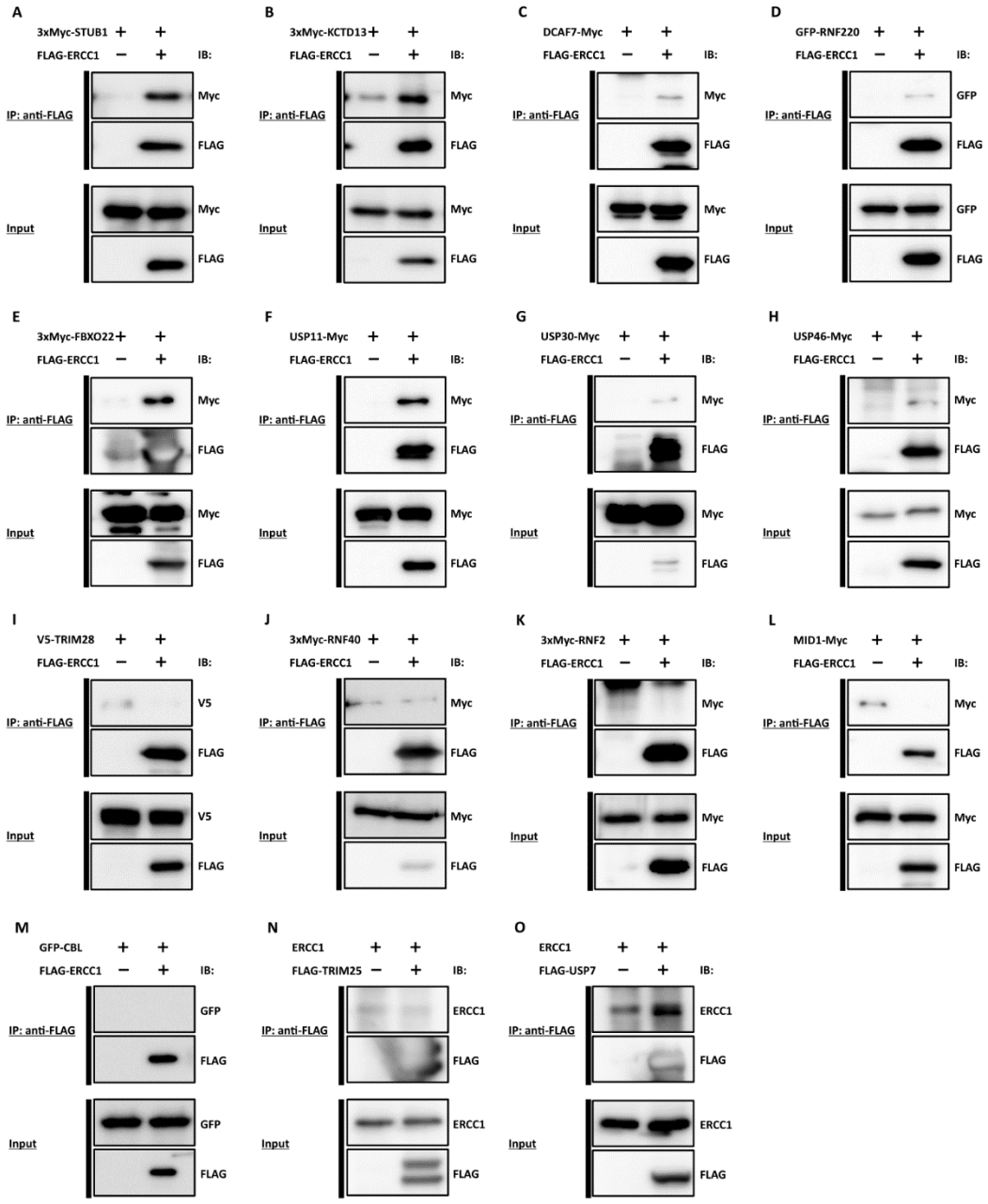

Figure.4 Co-immunoprecipitation experiments after transient expression of various candidate interactors and ERCC1.

An epitope-tagged version of various candidate interactors and FLAG-tagged or non-tagged ERCC1 were transiently co-expressed in HEK293T cells for 48 h. Cell lysates were precipitated by anti-FLAG or anti-Myc antibody resin and analyzed by western blotting with the indicated antibodies.

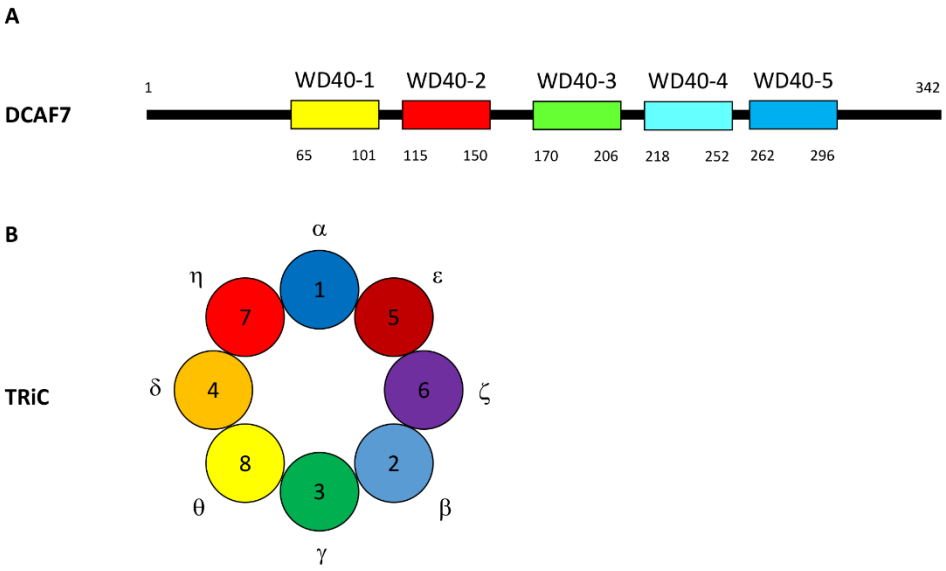

Figure. 5 Structures of DCAF7 and TRiC/CCT
(A) Domain structure of DCAF7/WDR68/HAN11. (B) Ring structure of TRiC/CCT complex

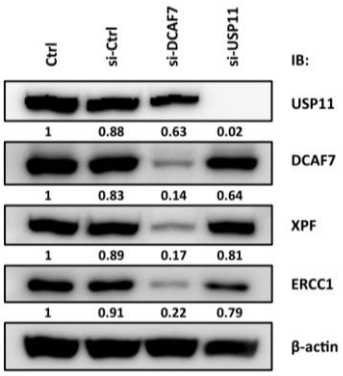

Figure. 6 DCAF7 depletion causes reduction of cellular levels of ERCC1 and XPF, while USP11 depletion diminishes only ERCC1 level.
U2OS cells were transfected with control siRNA, DCAF7 siRNA (#1) or USP11 siRNA and incubated for 72 h. Cell lysates were prepared and analyzed by western blotting with the indicated antibodies.

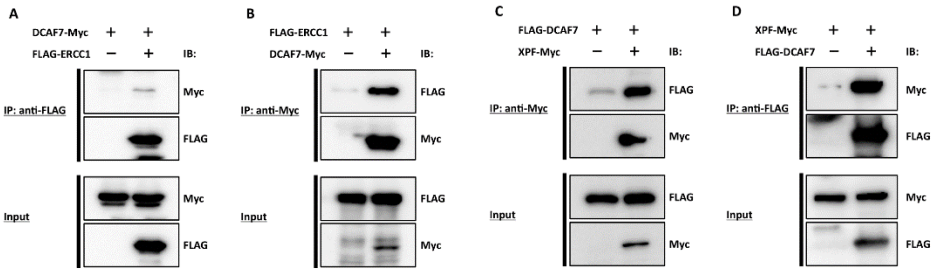

Figure 7. ERCC1-XPF binds to DCAF7

(A and B) DCAF7-Myc and/or FLAG-ERCC1 were ectopically expressed in HEK293T cells and cell lysates were immunoprecipitated by anti-FLAG antibody resin (A) or anti-Myc antibody resin (B). (C and D) FLAG-DCAF7 and/or XPF-Myc were expressed in HEK293T cells and precipitated by either anti-Myc (C) or anti-FLAG antibody resin (D). The precipitates were analyzed by western blotting with the indicated antibodies.

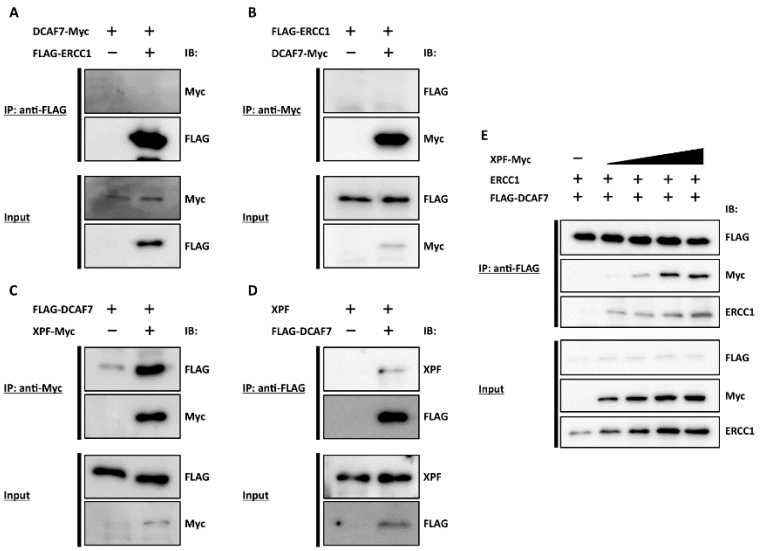

Figure 8. DCAF7 binds to XPF but not ERCC1

(A and B) DCAF7-Myc and/or FLAG-ERCC1 were ectopically expressed in XP2YO(SV) cells and cell lysates were immunoprecipitated by anti-FLAG antibody resin (A) or anti-Myc antibody resin (B). (C and D) FLAG-DCAF7 and/or Myc-tagged XPF (C) or non-tagged XPF (D) were expressed in XP2YO(SV) cells and precipitated by either anti-Myc (C) or anti-FLAG (D) antibody resin. (E) The same amounts of Non-tagged ERCC1 and FLAG-DCAF7 expression plasmids (0.65 μg each) were co-transfected with an increasing amount (0.65-5.2 μg) of XPF-Myc expression plasmid into XP2YO(SV) cells. The total amount of DNA was adjusted by empty vector pEF6/Myc-His. After 48 h, cell lysates were prepared and immunoprecipitated by anti-FLAG antibody resin. Each sample was analyzed by western blotting with the indicated antibodies.

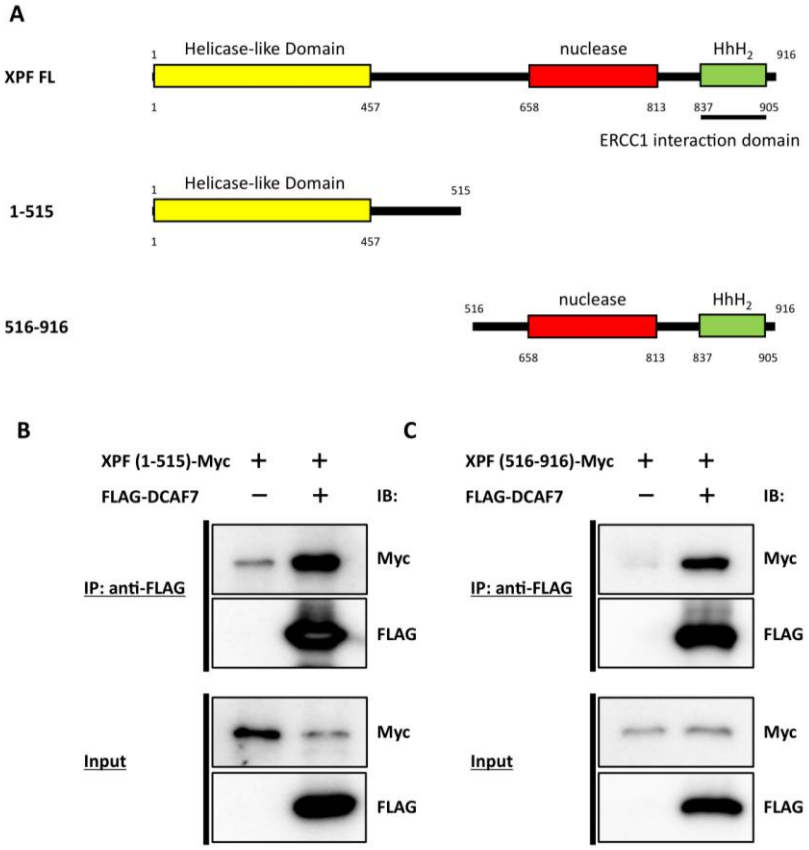

Figure 9. DCAF7 interacts with both N-terminal or C-terminal half of XPF.
(A) A schematic illustration of two kinds of XPF deletion mutants. (B and C) FLAG-DCAF7 and XPF(1-515)-Myc or XPF(516-916)-Myc were ectopically expressed in XP2YO(SV) cells and cell lysates were immunoprecipitated by anti-FLAG antibody resin. The precipitates were analyzed by western blotting with the indicated antibodies.

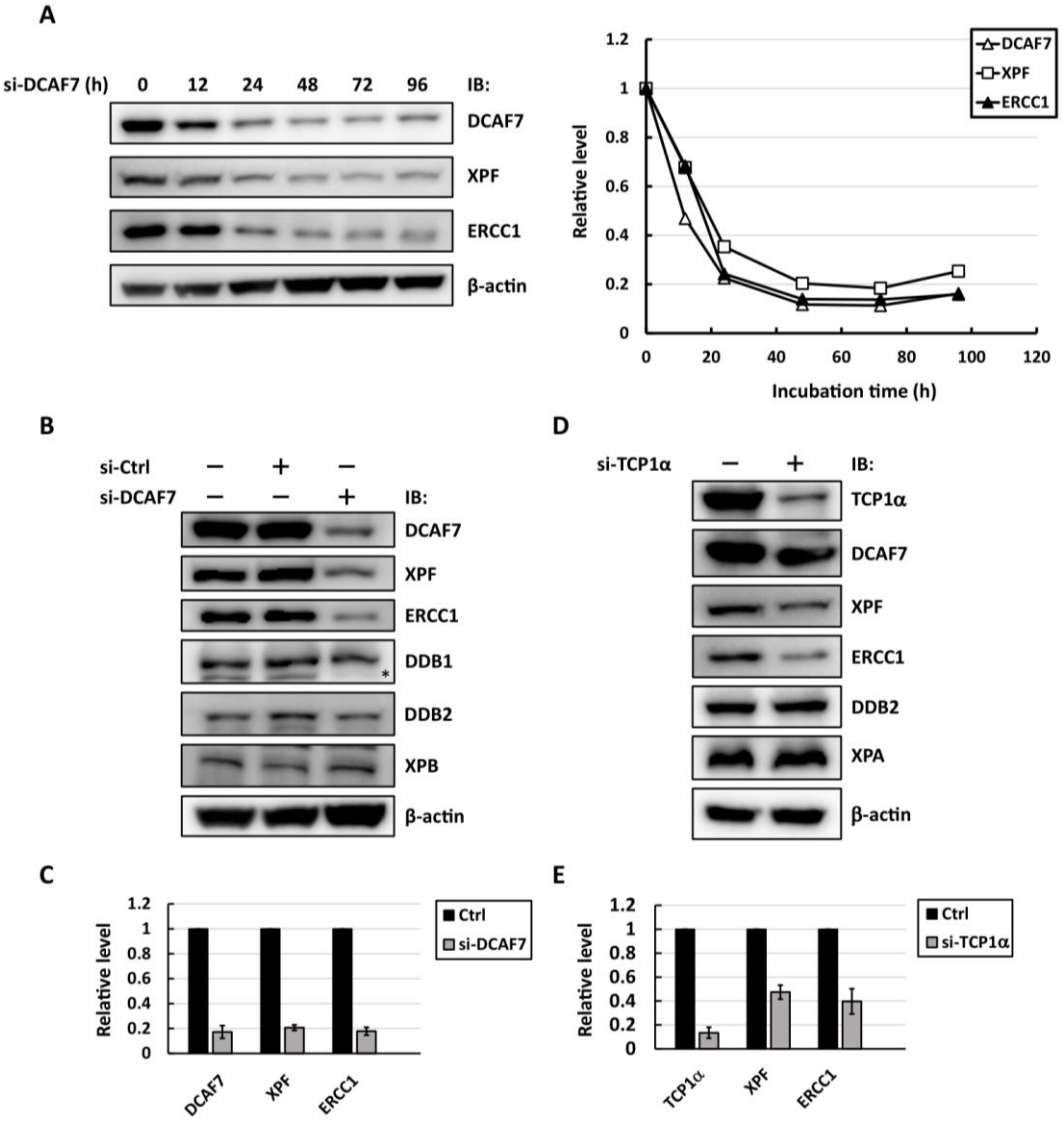

Figure 10. Depletion of DCAF7 reduces the cellular levels of ERCC1-XPF.
(A) U2OS cells were transfected with DCAF7 siRNA (#1) and incubated for the indicated period of time. After cell lysis, each sample was analyzed by western blotting with the indicated antibodies (left panel). An asterisk indicates non-specific bands. The signal intensity of each band was quantified and adjusted using internal control β-actin (right panel). (B - E) U2OS cells were transfected with either control siRNA or DCAF7 siRNA (#1) (B) or TCP1α siRNA (#1) (C). After 72 h, cell lysates were prepared and analyzed by western blotting with the indicated antibodies. The impacts of DCAF7 or TCP1α knockdown on ERCC1-XPF level were tested three times, and the mean and SD were shown in (D) or (E), respectively.

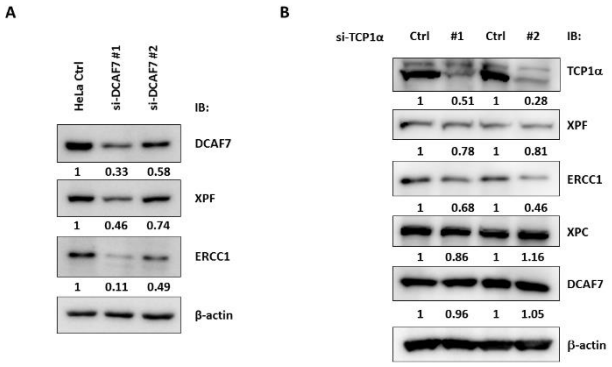

Figure 11. Depletion of DCAF7 reduces the cellular levels of ERCC1-XPF.
(A) HeLa cells were transfected with DCAF7 siRNA #1 or #2 as described in the "Materials and Methods" and incubated for 72 h. Cell lysates were prepared and analyzed by western blotting with the antibodies specific for DCAF7, XPF or ERCC1. β-actin was used as internal control. (B) U2OS cells were transfected with TCP1α siRNA #1 or #2 (see the "Materials and Methods") and lysed after 72-h incubation. Cell lysates were analyzed by western blotting with the indicated antibodies.

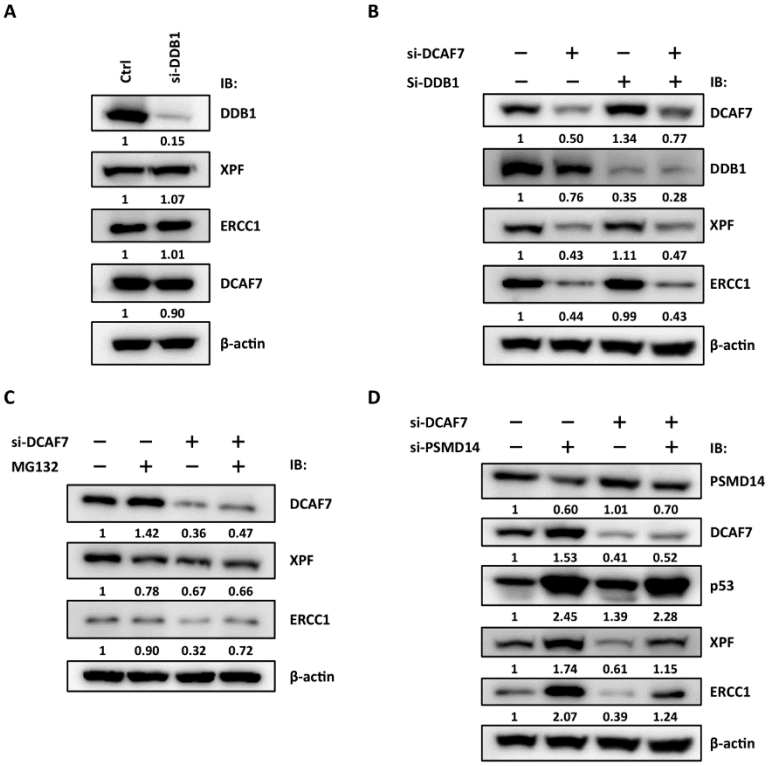

Figure 12. DCAF7-mediated regulation of ERCC1-XPF level is independent of Cul4-DDB1 E3 ligase and 26S proteasome.
(A and B) U2OS cells were transfected with DDB1 siRNA (A) or various combinations of control siRNA, DDB1 siRNA and DCAF7 siRNA (#1) (B) and incubated for 72 h. (C) U2OS cells were transfected with DCAF7 siRNA (#1) and incubated for 12 h. After addition of MG-132 (final 10 μM) or DMSO, the cells were further incubated for 12 h. (D) U2OS cells were transfected with control siRNA, PSMD14 siRNA or/and DCAF7 siRNA (#1) and incubated for 72 h. Cell lysates were prepared and analyzed by western blotting with the indicated antibodies. The relative band intensities adjusted using internal control β-actin were shown below each band.

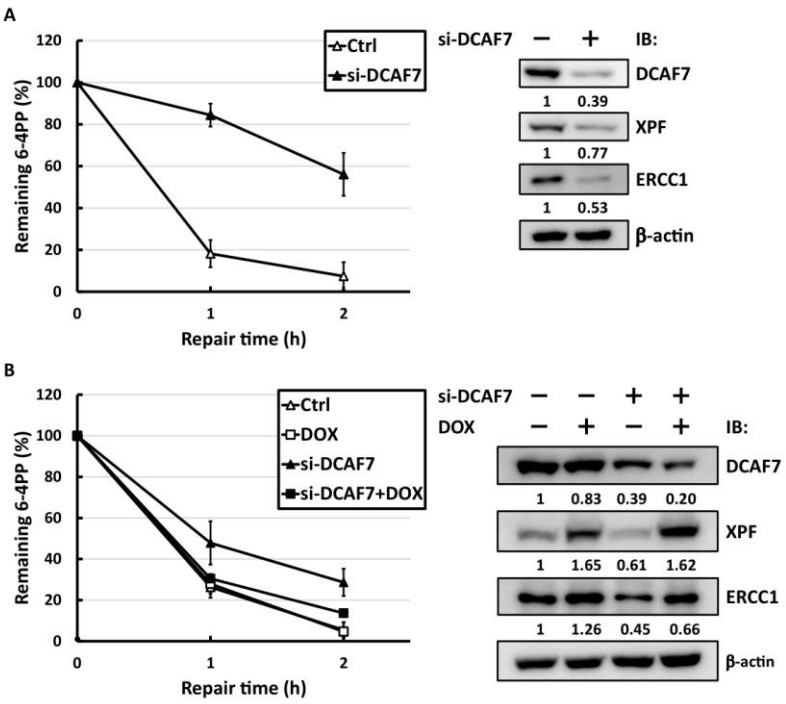

Figure 13. Depletion of DCAF7 suppresses the cellular activity of 6-4PP repair.
(A) HeLa cells were transfected with DCAF7 siRNA (#1) and incubated for 72 h. The cells were irradiated with 10 J/m2 of UV-C and further incubated for 1 or 2 h. Genomic DNA was purified from each sample and analyzed for the repair kinetics of 6-4PP using ELISA. Each point represents the mean of three experiments and bars indicate the SD (left panel). Knockdown of DCAF7 and subsequent downregulation of ERCC1-XPF were also monitored by western blotting of cell lysates prepared from the same samples (right panel). The relative band intensities adjusted using internal control β-actin were shown below each band. (B) Flp-In T-REx 293/FLAG-XPF-6xHis cells were transfected with DCAF7 siRNA and incubated for 48 h. Doxycycline was added to the cell culture at a final concentration of 1 μg/ml and cells were further incubated for 24 h. After irradiation with 10 J/m2 of UV-C, the repair kinetics of 6-4PP (left panel) and the protein levels of DCAF7, XPF and ERCC1 (right panel) were determined as described in (A).

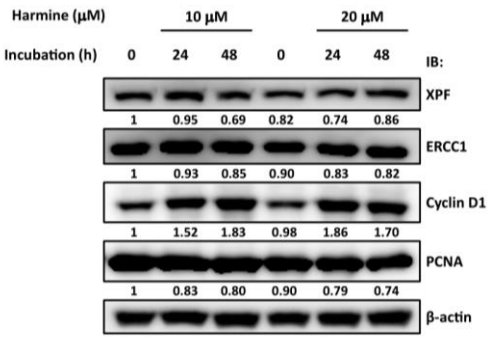

Figure 14. DYRK1A kinase inhibitor Harmine doesn't significantly affect the cellular level of ERCC1-XPF

U2OS cells were incubated with 10 mM or 20 mM Harmine, a DYRK1A kinase inhibitor, for 24 or 48 h. Cell lysates were prepared and analyzed by western blotting with the indicated antibodies.